# NACA

# RESEARCH MEMORANDUM

A STUDY OF FUEL-NITRIC ACID REACTIVITY

By Charles E. Feiler and Louis Baker, Jr.

Lewis Flight Propulsion Laboratory Cleveland, Ohio

# NATIONAL ADVISORY COMMITTEE FOR AERONAUTICS

WASHINGTON

April 6, 1956 Declassified February 26, 1958

# NATIONAL ADVISORY COMMITTEE FOR AERONAUTICS

# RESEARCH MEMORANDUM

A STUDY OF FUEL-NITRIC ACID REACTIVITY

By Charles E. Feiler and Louis Baker, Jr.

# SUMMARY

The relative reactivities of six fuels with red fuming nitric acid (19 percent NO<sub>2</sub>) were determined in a 40-pound-thrust rocket engine with rapid liquid-phase mixing. The combustion-chamber characteristic length required to obtain 97 percent of maximum experimental characteristic exhaust velocity was used as the measure of reactivity. Hydrazine, trimethyl-trithiophosphite, furfuryl alcohol, unsymmetrical dimethyl-hydrazine, allylamine, and o-toluidine were studied; reactivity decreased in that order.

A swirl-cup-type injector was used. Injector spray pattern and mixing efficiency were determined. The swirl-cup pressure drop depended strongly on the nature of the fuel-acid mixture and was assumed to be a measure of the vigor of the reaction occurring in the cup.

One-inch-diameter chambers of various lengths were used. Two of the fuels were also studied in  $1\frac{1}{2}$ - and 2-inch-diameter chambers. Reactivities are shown to be dependent on the acid-fuel ratio. Reactivities, injector-cup pressure drops, and ignition delays are compared and discussed.

## INTRODUCTION

The selection of rocket propellants for a specific purpose would be aided if, in addition to thermodynamic and physical data, there were available some index of reaction rate. Such an index would also be of value in the design of the smallest, lightest combustion chambers consistent with efficient combustion.

Several investigations have been made to determine reactivities or conversion rates in rocket combustion chambers. In one, the characteristic exhaust velocity c\* was measured as a function of chamber length for several fuels with liquid oxygen as the oxidizer (ref. 1). (The symbols used in this report are defined in appendix A.) The study was primarily for the purpose of correlating conversion rates with flame speeds and slow oxidation rates. Flame speeds and slow oxidation rates are not

NACA RM E56A19

necessarily related to combustion processes that occur in rocket engines; however, qualitative correlations were obtained. Similar data have also been used in the evaluation of injector configurations for the system, white fuming nitric acid (WFNA) and JP-3 fuel (ref. 2).

In another investigation the static-pressure profile along a tubular engine was determined, and from this, reaction rates were inferred (ref. 3). WFNA-ammonia and WFNA-hydrazine systems were studied with a number of injector configurations. Similar data have been interpreted to give a minimum required residence time for the combustion of gaseous methane and oxygen (ref. 4).

This report describes an investigation of the relative reactivities of several fuels with red fuming nitric acid (RFNA) under conditions where the effect of liquid-phase mixing is minimized. The combustion-chamber characteristic length L\* required to obtain 97 percent of the maximum experimental characteristic exhaust velocity c\* was used as the measure of reactivity. A swirl-cup-type injector was used because this type has been shown to produce very rapid liquid-phase mixing (ref. 5). The mixing efficiency and spray pattern of the injector were determined.

Six fuels, representative of several classes, were studied using RFNA (19 percent NO<sub>2</sub>) as the oxidizer. The experiments were conducted in a nominal 40-pound-thrust rocket engine. The characteristic length L\* of the combustion chamber was varied by using different lengths of linch-diameter pipe. Two of the fuels were also studied in  $1\frac{1}{2}$ - and 2-inch-diameter chambers to determine the effect of diameter on the general level of performance and on the reactivities of the fuels. The ratings of the fuels, based on data for c\* and L\* and cup pressure drop, are compared.

An attempt was made to interpret the results of this study assuming that the conversion of NO to  $\rm N_2$  is an important rate-determining step in the final stages of combustion involving nitric acid (refs. 6 and 7).

# APPARATUS AND PROCEDURE

# Rocket Engine

A cross-sectional view of the rocket engine and injector is shown in figure 1.

<u>Injectors</u>. - The injectors were of a swirl-cup type similar to that reported in reference 8. Propellants entered the mixing cup tangentially at an inlet angle of  $10^{\circ}$ . The cross-sectional area of the mixing cup was 4 times the sum of the cross-sectional areas of the inlet orifices. The cup length was chosen for approximately 1 millisecond of residence time based on the calculated velocity of unreacted propellants. Two injectors

3884

with different inlet-orifice diameters were required to permit operation over a wide range of mixture ratios. The injector heads were constructed of stainless steel and contained a pressure tap leading directly to the chamber.

Separate experiments were conducted to determine the mixing efficiencies and spray patterns of the injectors. The details of these experiments are presented in appendix B. The results indicate that mixing was largely excluded as a factor in the present study and that the data represent primarily evaporation and chemical-reaction rates. Studies of the spray patterns indicated an almost uniform distribution with a cone angle of about  $37^{\circ}$ .

Chambers. - Uncooled chambers were made of extra-heavy seamless steel pipe having 1-,  $1\frac{1}{2}$ -, and 2-inch nominal diameters. In addition, transparent chambers of cast acrylic resin were used for a photographic study. These had a wall thickness of 1/4 inch and inside diameters of 1/4, and 2 inches. Figure 1 shows a 1-inch chamber only. Adaptors were used to fit the wider chambers to the injector. When adaptors were used, there was a prechamber space 2/3-inch long with a 1-inch diameter. This space had a characteristic length of 6 inches. The 1-,  $1\frac{1}{2}-$ , and 2-inch-diameter chambers had characteristic lengths of 8.1, 19.9, and 33.3 inches, respectively, per inch of chamber length.

<u>Nozzles.</u> - Stainless-steel water-cooled nozzles having a convergent section only were used. The nozzles were constructed with steps to accommodate the various chamber diameters. The injector, chamber, and nozzle were bolted together and sealed by copper or aluminum gaskets at both ends of the chamber. The entire assembly was directed downward.

# Flow System and Operation

The flow system of the test rig was similar to those used in other experimental rocket setups. The two propellant tanks could be pressurized independently to about 850 pounds per square inch gage. A pneumatically operated firing valve permitted flow of both propellants to begin simultaneously. The initial flow rates were about twice the steady-state values. Because of the high initial flow rates, the ignition process was affected and hard starts were encountered with furfuryl alcohol, allylamine, and o-toluidine. In order to prevent such hard starts, these fuels were preceded by a 3- to 5-cubic-centimeter slug of 82 percent hydrazine, which was fed directly into the firing valve through a short length of vertically mounted tubing. The other fuels showed smooth-starting characteristics over the entire range of acid-fuel ratios.

Without starting fuel the total running time was usually 1 to 2 seconds. When starting fuel was used, the running time was increased to about 3 seconds to ensure the complete removal of the starting fuel. Running time on starting fuel ranged from 0.2 to 0.5 second. Transition from starting fuel to running fuel could sometimes be detected in the flow and chamber-pressure records. All the runs were long enough so that the flow rates and chamber pressure reached constant values.

In order to purge the injector and chamber at the end of each run, high-pressure helium was automatically admitted downstream of the firing valve just as the valve closed.

#### Instrumentation

Duplicate measurements were made of all primary variables. Propellant flow rates were measured both by rotating-vane flowmeters and by orifices in conjunction with strain-gage differential-pressure transducers. In order to protect the pressure transducer in the acid line from the corrosive action of the acid, a fluorocarbon oil was placed in the lines connecting the orifice and the transducer chamber. The oil (sp. gr., 1.95), being heavier than acid, prevented contact between the acid and the sensitive instrument diaphragms. Although some  $\mathrm{NO}_2$  was absorbed by the oil, no corrosion of the metal diaphragm was observed over a period of a year.

The chamber pressure was measured by two strain-gage static-pressure transducers placed 18 and 30 inches from the injector on a single pressure tap line. The pressure tap line was 1/4-inch-diameter stainless-steel tubing and was provided with a slight helium bleed to keep it unblocked and to prevent possible explosions due to propellant entry on starting.

The outputs of all instruments were recorded on a multichannel galvanometer-type oscillograph. The flow rates and pressures used were averages of the duplicate measurements. The deviations between flow rates obtained from the rotating-vane instrument and the orifice-straingage combination averaged 0.003 pound per second for the acid and 0.002 pound per second for the fuel. The deviations between chamber-pressure measurements from each of the strain gages averaged 2.2 pounds per square inch.

The nozzle diameter was measured before and after each series of runs, and an average of these two values was used. Propellant temperatures were measured with a mercury thermometer at each loading of the tanks.

# Fuels and Acids

The acid used throughout the study was a red fuming nitric acid containing 19 percent  $\mathrm{NO}_2$  and 2 percent water. The six fuels used were 92.2 percent hydrazine, commercial-grade trimethyl-trithiophosphite (TMTP), commercial-grade furfuryl alcohol, commercial-grade unsymmetrical dimethyl-hydrazine (UDMH), commercial-grade allylamine, and chemically pure otoluidine. In the mixing efficiency tests, 18.8 percent  $\mathrm{HNO}_3$  and  $\mathrm{18.2}$  percent  $\mathrm{NaOH}$  in water were used.

### Treatment of Data

The characteristic length L\* was calculated from chamber volume/nozzle throat area; characteristic exhaust velocity c\* was calculated from (chamber pressure)(nozzle throat area)/total flow rate. The L\* corresponding to maximum c\* is difficult to locate accurately because the experimental curves are almost horizontal over a wide range of L\* near the maximum. For this reason the L\* for comparison was chosen as that at which c\* reached 97 percent of its maximum value. At this point L\* the curves are steep enough to give a well-defined value of L\*.

Values of  $\beta$  (o/f)/(o/f)<sub>stoichiometric</sub> of 0.55, 0.65, 0.80, 1.0, and 1.25 were selected for comparing the various fuels. The acid-fuel weight ratios o/f corresponding to these  $\beta$  values are shown for each fuel in table I. The choice of these values was limited by the range of the data, which in some cases did not extend to the extreme values. Special significance is attached to  $\beta$  of 0.80 since it corresponds approximately to the o/f of maximum c\* for all the fuels.

Theoretical performance data for the exact acid composition used in this study were not available; however, some applicable data were found. The data for hydrazine and furfuryl alcohol are from reference 9. The data for UDMH are from reference 10. It was necessary to correct the hydrazine data for the effect of about 8 percent water. The correction was based on the data of reference 9 and reduced the c\* values for anhydrous hydrazine by 1.2 percent.

## RESULTS

The basic measured and calculated data are shown in table II for each fuel. The flow-rate values are given to three decimal places; how-ever, in some cases four places were used to compute c\* and o/f. Runs in which screaming (high-frequency sound due to combustion oscillations)

5884

was heard are marked. In every case when screaming was heard, the chamber-pressure record was smooth and free from random disturbances otherwise present.

Figure 2 shows typical  $c^*$ - o/f curves for each fuel at the L\* giving the highest  $c^*$ . These data are for l-inch-diameter chambers and are representative of data obtained at other L\* values. The experimental points show the reproducibility of the data to be very good. Theoretical  $c^*$  curves for three of the fuels are also shown in figure 2.

# Combustion Characteristics of the Fuels

Three of the fuels, hydrazine, TMTP, and UDME, were very smooth in operation giving no hard starts or audible screaming. Furfuryl alcohol screamed consistently in chambers having an L\* of 50 inches and greater over the entire o/f range studied. Some intermittent screaming was observed with allylamine and o-toluidine in the longer chambers. This usually occurred near the end of a run, so that it was usually possible to obtain data when there was no screaming. No difference was observed between c\* values for screaming and nonscreaming runs. This is illustrated in figure 2 where data points for both conditions are shown for furfuryl alcohol and o-toluidine. TMTP produced hard deposits in the nozzle throat. Both furfuryl alcohol and o-toludine formed copious carbon deposits in the chambers.

# Fuel Ratings

In figure 3, c\* is shown as a function of L\* and o/f for each fuel. The curves are for l-inch-diameter chambers and are taken from smoothed c\* - o/f plots like those in figure 2. The  $\beta$  values at which the fuels are compared later are marked. From figure 3 it can be seen that the o/f giving a maximum c\* generally increases as L\* is increased.

In figure 4, the fuels are compared at a  $\beta$  of 0.80;  $L_{97}^{\star}$  points are shown. These curves are similar in form to those obtained at the other values of  $\beta$ . The characteristic exhaust velocities  $c^{\star}$  for allylamine and o-toluidine did not reach a maximum even at an  $L^{\star}$  of 100 inches. As an approximation, maximum  $c^{\star}$  was taken as that at an  $L^{\star}$  of 100 inches; therefore the  $L_{97}^{\star}$  values are a minimum for these two fuels. The results of the evaluation of  $L_{97}^{\star}$  are given in table III as a function of  $\beta$  for the six fuels. The maximum  $c^{\star}$  values are listed in table IV.

The fuels in order of increasing  $L_{97}^*$  and hence decreasing reactivity are hydrazine, TMTP, furfuryl alcohol, UDMH, allylamine, and o-toluidine.

It is apparent from table III that the reactivity decreases as the stoichiometric o/f increases. On the fuel rich side, the  $L_{97}^{*}$  values generally increase for a given fuel as  $\beta$  increases. The dependence on the relative amounts of acid and fuel present is shown in figure 5 in which all of the  $L_{97}^{*}$  values in table III are plotted against the corresponding o/f. The data fall into two groups with allylamine and o-toluidine separated from the remaining four fuels.

# Pressure in the Mixing Cup

The flow rates observed during live runs were much lower than those expected from cold-flow tests. This effect was apparently due to a large pressure drop in the injector mixing cup resulting from liquid-phase reaction. Cup pressure drop is a measure of the amount of liquid-phase reaction in the cup, since only a negligible pressure drop would have resulted from fluid friction alone. The cup pressure drop was calculated using the equation for flow through an orifice. Details of the calculation are given in appendix C. Calculated values of the cup pressure drop are shown in figure 6 as a function of o/f. The values are corrected to a uniform flow rate of 0.2 pound per second (see appendix C). The pressure drops tend toward a common value independent of the fuel as o/f is increased.

## Effect of Chamber Diameter

The effect of chamber diameter on the general level of performance and on the reactivities of the fuels was investigated. Two fuels, hydrazine and UDMH, showing widely different reactivities in the 1-inch-diameter chambers were studied in  $l^{\frac{1}{2}}$ - and 2-inch-diameter chambers. Characteristic exhaust velocity  $c^{*2}$  for each diameter is shown as a function of L\* in figure 7(a) and as a function of chamber length in figure 7(b). Data for  $\beta$  equal to 0.80 only are shown as they are typical of the data for all  $\beta$  values. From figure 7(a), the L\* corresponding to maximum  $c^*$  increased with diameter for both fuels. From figure 7(b) the chamber length corresponding to maximum  $c^*$  decreased with diameter for UDMH, while no trend was observed for hydrazine. The maximum  $c^*$  increased slightly with diameter for UDMH, while no trend was observed for hydrazine.

 $L_{97}^*$  values are shown in table V as functions of diameter for hydrazine and UDMH.  $L_{97}^*$  increases with both diameter and  $\beta$ .

## DISCUSSION

# Effect of Chamber Diameter

An analysis of the data of table V showed that an essentially constant difference exists between the L37 values of each of the larger chambers and the 1-inch chambers. The average differences in 197 values, shown in table VI, are 19.1 inches between the  $1\frac{1}{2}$ - and 1-inch diameters and 42.9 inches between the 2- and 1-inch diameters. As discussed in appendix B, the injectors produced a conical spray pattern. It was assumed that the chamber volume outside the spray cone did not contribute to the effective combustion volume. This ineffective combustion volume was calculated from the cone angle and chamber geometry. The ineffective volume was converted to an equivalent L\* for each of the chamber diameters. The difference in L\* values thus obtained for the various chamber diameters were of the same order of magnitude as those observed experimentally. The differences may be applied as a correction to the 197 values obtained with the larger-diameter chambers resulting in approximately the same Ly values for all diameters. This result indicates that in the range of diameters studied there is little effect of chamber diameter on the observed reactivities.

# Correlation of Reactivity with Initial NO Concentration

From the relation between  $L_{97}^{*}$  and o/f shown in figure 5, it appears that, in a very general way, the reactivity of a combination containing unit mass of fuel depends on the amount of acid present; that is, even on the fuel rich side, the reactivity decreases as the acid concentration is increased. For some of the fuels the differences in reactivity between fuels were less than those produced by changes in the acid-fuel ratio. It seems reasonable therefore to relate reactivity to some function of acid concentration in the reactant mixture.

It has been postulated that in oxidation reactions involving nitric acid or  $\mathrm{NO}_2$ , where NO is an intermediate, the steps involving NO are slow and rate-determining. It has been found that the measured flame speeds of NO-hydrocarbon mixtures were about 1/10 those of oxygen-hydrocarbon mixtures with hydrocarbons such as ethane, ethylene, and acetylene (ref. l1). Other evidence indicates that higher temperatures are required to propagate NO supported flames than flames supported by  $\mathrm{O}_2$  or  $\mathrm{NO}_2$  (ref. l2). Also, analysis of the primary cone of a premixed gaseous nitric acid-hydrocarbon flame showed that nearly all the nitrogen is recovered as NO (ref. l3).

An attempt was therefore made to correlate the experimental data with some function of NO concentration. It was assumed that the following reaction occurs very rapidly to form intermediates and products as shown:

Fuel +  $\text{HNO}_3$  ( $\text{NO}_2$ )  $\rightarrow$  NO +  $\text{CO}_2$  + CO + C +  $\text{H}_2\text{O}$  +  $\text{H}_2$  +  $\text{N}_2$  +  $\text{P}_2\text{O}_5$  +  $\text{SO}_2$ 

All the nitrogen in the acid has been assumed to form NO. The other species are formed, where applicable, from the fuel. For each mixture ratio, the initial mole fraction of NO (moles NO/total moles) was calculated. Whether  $\mathrm{CO}_2$ ,  $\mathrm{CO}$ , or C and  $\mathrm{H}_2\mathrm{O}$  or  $\mathrm{H}_2$  is formed is not known but has no effect on the total number of moles. It was necessary, however, to assume that the amounts of  $\mathrm{O}_2$ ,  $\mathrm{OH}$ ,  $\mathrm{H}$ ,  $\mathrm{CH}$ , and so forth present after the initial reaction are negligible. Using experimental chamber pressures each mole fraction was converted to a partial pressure of NO. The initial partial pressure of NO represents the amount of NO that must react to carry the reaction to completion. These pressures are plotted as a function of  $\mathrm{L}_{97}^*/\mathrm{c}_{97}^*$  for each fuel in figure 8. The ratio  $\mathrm{L}_{97}^*/\mathrm{c}_{97}^*$  has the dimensions of time and is shown in appendix D to be roughly proportional to the residence time of the propellants from injection to the point of 97 percent maximum  $\mathrm{c}^*$ .

The shapes of the curves for the individual fuels in figure 8, with the possible exception of hydrazine, are inconsistent with any rate law based on a single reaction. If, at the final state (97 percent maximum c\*), the partial pressure of NO is the same value for all mixtures, and if the disappearance of NO followed a first, second, or higher order dependence, the curves would be concave to the pressure axis.

The curves for furfuryl alcohol, UDMH, and allylamine approach a common limiting line at higher initial NO concentrations. The slope of the limiting line is small and may represent the thermal decomposition of NO. At lower initial NO concentrations the slopes are higher suggesting that NO is reacting with fuel fragments. Thus the shape of the curves may be explained on the basis of two competing reactions, one, the thermal decomposition of NO, which is slower, and the other, the reaction of NO with fuel fragments, which is faster. The curve for hydrazine does not suggest such a mechanism; however, the initial partial pressures of NO in all runs with hydrazine were quite low. The TMTP and o-toluidine curves are not consistent with such a conclusion.

The slope of the limiting line in figure 8 was found to be  $3.9\times10^3$  pounds per square inch per second. The calculation of the slope includes a correction of the time base of figure 8 as shown in appendix D. The rate of thermal decomposition of NO, calculated from experimental data, increased from  $6.5\times10^3$  to  $4.6\times10^4$  pounds per square inch per second as the temperature was increased from  $3500^\circ$  to  $4100^\circ$  R (ref. 6). Thus the slope of the limiting line is of the same order of magnitude as the calculated rate of thermal decomposition of NO.

The validity of this correlation is, of course, limited by the uncertainty of the final concentration of NO and the assumptions regarding the fate of the fuel atoms.

Comparison of Cup Pressure-Drop, L\*, and Ignition-Delay Values

The values of the steady-state pressure drop in the mixing cup were shown in figure 6 as a function of o/f for each fuel. The propellants are in the mixing cup for about 1 millisecond so that a high cup pressure drop indicates appreciable early reaction. From figure 6 it is apparent that the pressure drop is fuel dependent for fuel-rich mixtures. Cuppressure-drop values and  $L_{97}^{\star}$  values are compared at a  $\beta$  of 0.65 in table VII. With the exception of furfuryl alcohol, cup-pressure-drop ratings follow the same trend as  $L_{97}^{\star}$  ratings.

The ignition-delay values of the fuels also shown in table VII were not all obtained under comparable conditions; however in general, the fuels are divided into two groups according to their ignition delays. Fuels having short ignition delays, hydrazine, TMTP, and UDMH, have the highest cup-pressure-drop values. Fuels having long ignition delays have the lowest cup-pressure-drop values.

It is to be expected that cup pressure drops and ignition delays should correlate because both characterize the initial processes in the combustion reaction. However,  $L_{97}^{\star}$  is a measure of the over-all conversion rate and characterizes the entire combustion process. Moreover, the correlation with initial NO concentration suggests that  $L_{97}^{\star}$  may be largely determined by the final stages of the combustion process. The observation that  $L_{97}^{\star}$  ratings and cup-pressure-drop ratings follow the same trend indicates that generally a combustion reaction which is vigorous in its early stages also will have a high over-all conversion rate.

As shown in figure 6, the cup-pressure-drop values for all the fuels seem to approach a common value of about 80 pounds per square inch at high o/f ratios. This value is considerably higher than would be expected from fluid friction alone. It may be due to thermal decomposition of the acid, with the necessary heat being supplied by transfer upstream from the combustion process. If it were caused entirely by reaction of fuel and acid in the cup, it would be expected that different values would be obtained for the various fuels such as were obtained at lower o/f ratios.

# Over-All Combustion Efficiency

Theoretical performance curves for three of the fuels were shown in figure 2. The following table shows the percent of theoretical  $c^*$  obtained at the o/f of experimental peak  $c^*$ .

Fuel	L*	Percent of theoretical c*							
		Frozen expansion	Equilibrium expansion						
Hydrazine Furfuryl	40	92.4							
alcohol	50 75	94.3	90.5						

As discussed previously, the acid composition used in the calculation of theoretical c\* did not correspond exactly to that used in the experimental study. Within this limitation the experimental efficiency is about the same for all three fuels. The experimental data are uncorrected for heat lost to the walls. An estimate of such heat loss showed that it could vary from about 3 percent in an L\* of 30 inches to about 8 percent in an L\* of 100 inches for the 1-inch-diameter chambers. It appears therefore that the relatively low efficiency can be largely accounted for by heat transfer to the chamber walls.

## CONCLUDING REMARKS

The concept of a volume required to complete a reaction has been used to classify six fuels with respect to their reactivities. The importance of data of this kind can be illustrated by the results of some performance measurements on a 5000-pound-thrust NHz-RFNA engine having an L\* of 17.5 inches (ref. 14). In spite of the small L\*, high specific impulse was obtained indicating that NHz has a high reactivity. The effect of adding UDMH to the NHz was then studied. Although UDMH has a higher theoretical performance than NHz, the addition of 30 percent UDMH to the NHz lowered the specific impulse 13 percent. This is not surprising in the light of the present research since an L\* of about 75 inches was required to obtain maximum performance with UDMH.

It is possible that finer discrimination between fuel-oxidant systems could be obtained by using a continuously variable L\* engine. This would improve the internal consistency of the data by eliminating cross plots. It would also allow the entire L\* range to be scanned.

# SUMMARY OF RESULTS

Using the chamber characteristic length L\* required to obtain 97 percent of maximum experimental characteristic exhaust velocity c\* as an index, the relative reactivities of six fuels with RFNA were determined. The experiments were conducted in a 40-pound-thrust rocket engine using a swirl-cup injector which gave about 70-percent-complete liquid-phase mixing. The results of the investigation may be summarized as follows:

- 1. The reactivities of the fuels were found to decrease in the following order: Hydrazine, trimethyl-trithiophosphite, furfuryl alcohol, unsymmetrical dimethylhydrazine, allylamine, and o-toluidine. The latter two fuels had considerably lower reactivities than the remaining four fuels.
- 2. As acid-fuel ratio  $\mbox{o/f}$  was increased, the reactivities of the fuels generally decreased.
- 3. From an analysis of the effect of stoichiometry, it appears that for at least three of the fuels two reactions involving NO may be important. The reaction of NO with fuel fragments is the faster reaction; the thermal decomposition of NO is slower.
- 4. The pressure drop through the mixing cup appeared to be a measure of the extent of liquid-phase reaction. This pressure drop followed the same general trend as ignition delay.
- 5. The chamber diameter had no effect on the relative ratings of two fuels studied as functions of diameter.

Lewis Flight Propulsion Laboratory
National Advisory Committee for Aeronautics
Cleveland, Ohio, January 19, 1956

# APPENDIX A

The following symbols are used in this report:

- A area, sq in.
- Cd discharge coefficient
- c\* characteristic exhaust velocity, pcAtg/wt, ft/sec
- g gravitational constant, 32.2 ft/sec<sup>2</sup>
- h ratio of average value of RT/M to value at nozzle entrance
- K flow constant,  $C_d^2A^22gp/144$ , (lb)(sq in.)/sec<sup>2</sup>
- L\* characteristic length,  $V_c/A_t$ , in.
- M molecular weight of combustion gases
- o/f acid-fuel ratio,  $w_o/w_f$
- p pressure, lb/sq in.
- R universal gas constant, ft-lb/lb-mole OR
- T combustion-chamber temperature, OR
- t residence time of combustion gases in chamber, sec
- V<sub>c</sub> combustion-chamber volume, cu in.
- ${
  m V_g}$  average specific volume of gases in combustion chamber, cu ft/lb
- w flow rate, lb/sec
- $w_{\rm T}$  total flow rate,  $w_{\rm O}$  +  $w_{\rm f}$ , lb/sec
- β weight fraction of stoichiometric o/f,  $\frac{o/f}{(o/f)_{stoichiometric}}$
- $\Gamma$   $\gamma \sqrt{\left(\frac{2}{\gamma+1}\right)^{\frac{\gamma+1}{\gamma-1}}}$
- γ specific-heat ratio
- ρ density, lb/cu ft

# Subscripts:

av aver**a**ge

c combustion chamber

cup injector mixing cup

f fuel

i nozzle inlet

o acid

p propellant tank

t nozzle throat

#### APPENDIX B

# INJECTOR CHARACTERISTICS

The injector was characterized by studies of its mixing efficiency and spray pattern.

#### Mixer

A separate apparatus (fig. 9) was used to study the mixing efficiency of the injector. The flow arrangement was identical to that in the injector except that the mixing cup was extended to a length of 6 inches with tubing having a 0.020-inch wall thickness. Iron-constantan thermocouples were spot-welded to the mixing tube at various stations. The entire mixer was enclosed by a heater so that the initial temperature of the block, which is the greatest heat sink, could be adjusted to minimize heat transfer. The extended tube was carefully insulated from the heater to avoid heat transfer from the heater to the mixing tube during a run.

# Efficiency of Mixing

The mixing efficiency of the injector was studied with dilute nitric acid and sodium hydroxide. Inasmuch as the reaction between a strong base and a strong acid is instantaneous and dependent only on the rate of mixing (ref. 5), the heat evolved by such a reaction can be used as an index of the completeness of mixing under adiabatic conditions. By following the temperature rise as a function of distance along the mixing tube, mixing efficiency can be determined (ref. 5). The temperature corresponding to complete mixing is calculable from thermodynamic data.

Smoothed data with three initial block temperatures are shown in figure 10. The upper curve corresponds to a high initial block temperature, which caused heat to be added to the stream resulting in a final temperature well above theoretical. The lower curve corresponds to a low initial block temperature for which the final temperature is below theoretical. The middle curve closely approximates the adiabatic case since the final temperature does reach theoretical. This is substantiated by the fact that the initial block temperature seems to be a reasonable average of the stream temperature in the region of the large block. From this curve it can be deduced that it requires 2.2 inches to achieve 97-percent-complete mixing. The extent of mixing at the distance corresponding to the end of the mixing cup in the rocket injector was found to be 70 percent. Whether the efficiency measured in the test mixer can be applied to mixing in the injector, under conditions where large amounts of heat and gas are evolved, may be somewhat questionable. A similar mixer,

under these conditions, gave an essentially complete reaction as fast as the reactants emerged from the mixer (ref. 15). It is thus concluded that mixing is largely excluded as a factor in the present study and that the data represent primarily evaporation and chemical-conversion rates.

# Studies of Spray Pattern

Experiments were conducted with plastic chambers of three diameters to determine how the reactants leaving the injector entered the chamber. Erosion patterns of the chambers using hydrazine as the fuel are shown in figure 11. The diameter measurements shown are averages of those made at a given station for two radial positions at right angles. The data for both positions are shown for the 2-inch chamber. Erosion was nearly symmetric about the circumference of the chamber indicating an almost uniform spray distribution.

The point of maximum erosion moved away from the injector as the diameter was increased. It was assumed that the point of maximum erosion represents the point of impingement of the burning spray from the injector on the chamber walls. These points are shown on a sketch of the chambers in figure 11. It can be seen that a straight line connecting them can be extended to the vicinity of the injector cup. This indicates that the injector spray under operating conditions is a cone having an included angle of about 37°. High-speed motion pictures, made with a framing camera, of the steady-state combustion showed that the chambers were not filled by luminous flame and that the cone angle was of the order of 40°. High-speed streak photographs showed considerable recirculation in the vicinity of the injector. Cold-flow tests using water gave a hollow-cone spray with an included angle of about 60°.

These results indicate that at least a part of the chamber volume upstream of the cone of burning may not contribute to the effective combustion volume.

# APPENDIX C

# CALCULATION OF PRESSURE DROP IN THE MIXING CUP

The calculation of cup pressure drop is possible because the mixing cup is the first point common to both the fuel and the acid flow lines. The calculation is based on the equation for orifice flow

$$w = C_{d}A \sqrt{\frac{2g\rho\Delta p}{144}}$$
 (C1)

If the friction factor is assumed constant, equation (Cl) may be applied to the entire flow line. Equation (Cl) may be squared and written both for the fuel line and the oxidant line as follows:

$$w_f^2 = K_f (p_{f,p} - p_{cup})$$
 (C2)

$$w_0^2 = K_0 (p_{0,p} - p_{cup})$$
 (C3)

where  $p_{f,p}$  and  $p_{o,p}$  are the fuel and oxidant tank pressures, respectively. Eliminating  $p_{cup}$  from equation (C2) and (C3),

$$\frac{w_0^2}{K_0} - \frac{w_f^2}{K_f} = p_{0,p} - p_{f,p}$$
 (C4)

Dividing by  $w_f^2$  and rearranging give

$$\frac{p_{0,p} - p_{f,p}}{w_{f}^{2}} = \frac{(o/f)^{2}}{K_{0}} - \frac{1}{K_{f}}$$
 (C5)

When  $(p_{0,p} - p_{f,p})/w_f^2$  is plotted against  $(o/f)^2$ , equation (C5) is a straight line of slope  $1/K_0$  and intercept  $-1/K_f$ .

The experimental program was conducted at a number, usually eight, of tank pressure settings for each fuel at each of the characteristic lengths studied. The experimental values of  $\mathbf{w}_0$ ,  $\mathbf{w}_f$ , and  $\mathbf{p}_c$  obtained with the various characteristic lengths at given tank pressure settings were averaged. The tank pressure settings and the average of each of the observed flow rates were then used to plot equation (C5). Such a plot for hydrazine is shown in figure 12. The corresponding plots for the other fuels also gave straight lines. From the measured slope and intercept, values of  $\mathbf{K}_0$  and  $\mathbf{K}_f$  were determined.  $\mathbf{K}_0$ ,  $\mathbf{K}_f$ ,  $\mathbf{p}_f$ ,  $\mathbf{p}_o$ ,  $\mathbf{p}_o$ ,  $\mathbf{p}_o$ ,  $\mathbf{p}_f$ ,  $\mathbf$ 

and  $w_0$  being known,  $p_{\rm cup}$  was calculated from equations (C2) and (C3). The two values of  $p_{\rm cup}$  agreed very closely, and their average was used to calculate the pressure drop by subtracting the chamber pressure from it;

$$\Delta p_{\text{cup}} = p_{\text{cup}} - p_{\text{c}} \tag{C6}$$

Since the average total flow rate  $w_T$  was not the same for each fuel, the cup-pressure-drop values were corrected to a common flow rate of 0.2 pound per second. In the absence of data on the flow of reacting mixtures the cup-pressure-drop values were assumed proportional to the total flow rate and adjusted to the reference value as follows:

$$\Delta p_{\text{cup,0.2}} = \frac{\text{O.2}}{\text{w}_{\text{T}}} \Delta p_{\text{cup,w}_{\text{T}}}$$
 (C7)

This constituted a relatively minor correction except in the case of hydrazine where the total flow rates were relatively low. The application of equation (C7) did not, however, change the relative order of the results.

# APPENDIX D

# RESIDENCE TIME IN CHAMBER

The residence time is given by equation (6-4) of reference 16

$$t = \frac{V_{C}}{w_{T}V_{g}}$$
 (D1)

 $v_{\rm g}$  may be eliminated from equation (D1) by using the perfect gas law  $v_{\rm g}$  = (RT/M)av/pc to give

$$t = \frac{p_c V_c}{w_T (RT/M)_{av}}$$
 (D2)

Since  $c^* = p_c A_t g/w_T$  and  $L^* = V_c/A_t$ ,

$$t = L^*c^* \frac{1}{g(RT/M)_{av}}$$
 (D3)

The  $(RT/M)_{aV}$  term is an average value for the entire chamber. It may be eliminated from equation (D3) by making use of an alternate expression for  $c^*$ , equation (3-32) of reference 16,

$$c^* = \frac{\sqrt{g_{\Gamma}(RT/M)_{\dot{1}}}}{\Gamma}$$
 (D4)

The  $(RT/M)_i$  in equation (D4) refers to conditions at the nozzle entrance. The c\* and L\* values involved in figure 8 refer to 97 percent maximum c\*. Because of the general similarity between the c\*-L\* curves for different fuels, it is reasonable to assume that  $(RT/M)_{av}$  is equal to the same fraction of  $(RT/M)_i$  for all cases since the nozzle conditions in all cases are comparable. Hence

$$(RT/M)_{av} = h(RT/M)_{i}$$
 (D5)

where h is a constant.

Combining equations (D3), (D4), and (D5) yields

$$t = \frac{L^*}{c^*} \frac{\gamma}{h\Gamma^2}$$

The value of  $\gamma/\Gamma^2$  is rather insensitive to the value of  $\gamma$  chosen. For  $\gamma$  values between 1.10 and 1.60,  $\gamma/\Gamma^2$  varies from 2.53 to 1.95. A value of 2.3 for  $\gamma/\Gamma^2$  was used. A value of unity was chosen for h. A value of h as low as 0.5 is unlikely; however, such a value would halve the rate obtained from the limiting line in figure 8.

#### REFERENCES

- 1. Raines, T., and Pisani, J.: Combustion Kinetics Investigation. Rep. RMI-487-F, Final Rep., Reaction Motors, Inc., Dec. 30, 1953. (Contract NOas 53-406-c.)
- 2. Datner, P. P., and Dawson, E. E.: Testing of Repetitive-Pattern Injectors in 1000-Lb Thrust Chambers with Chamber-to-Throat Area Ratios of 4.5 Using WFNA and JP-3. Rep. 555, Aerojet Eng. Corp., July 25, 1952. (Contract AF 33(038)-2733, Proj. MX-1079, E.O. No. 539-44.)
- 3. Samek, M. J., Baldwin, R. R., Cinnirella, E. O., and Kalil, E. O.: Combustion Kinetics in a Tube Motor. Rep. SPD 313, Final Rep., Special Proj. Dept., The M. W. Kellogg Co., Sept. 15, 1951. (Contract NOrd-10768 for U.S. Navy, Bur. Ord.)
- 4. Charyk, J. V., and Matthews, G. B.: Experimental Studies of Energy Release Rates in Rocket Motor Combustion Chambers. Rep. No. 191, Dept. Aero. Eng., Princeton Univ., Mar. 24, 1952. (Contract N6-ori-105, Task Order III, NR 220-038.)
- 5. Roughton, F. J. W., and Chance, B.: Investigation of Rates and Mechanisms of Reactions. Vol. 8 of Technique of Organic Chemistry, A. Weissberger, ed., Interscience Publ., 1953, p. 669.
- 6. Trent, C. H., and Datner, P. P.: A Study of Combustion of WFNA and JP-3 in Rocket Thrust Chambers. Rep. No. 628, Aerojet Eng. Corp., Nov. 15, 1952. (Contract AF 33(038)-2733, Item 30, Proj. MX-1079, E.O. No. 539-44.)
- 7. Wise, Henry, and Frech, Maurice F.: Reaction Kinetics of Rocket Propellant Gases. I. Rate of Decomposition of Nitric Oxide at Elevated Temperatures. Prog. Rep. No. 9-46, Jet Prop. Lab., C.I.T., Mar. 27, 1950. (Proj. No. TU2-1, Contract No. W-04-200-ORD-1482.)
- 8. Fredrickson, H., and Rice, P. J.: Second Progress Report on Rocket Motor Throttling. UMM-89, Eng. Res. Inst., Willow Run Res. Center, Univ. Mich., Jan. 1952. (USAF Contract W33-038-ac-14222, Proj. MX-794.)
- 9. Anon: 6000 Pound Thrust Jet Propulsion Unit. Pt. I Propellants Study. Final Rep., SPD-134, Spec. Proj. Dept., The M. W. Kellogg Co., Mar. 19, 1948. (USAAF Contract No. W-33-038-ac-13916.)
- 10. Camp, Clarence: Experimental Performance of Unsymmetrical Dimethylhydrazine Red Fuming Nitric Acid Rocket Propellant Combination. WADC Tech. Rep. 54-81, Wright Air Dev. Center, Wright-Patterson Air Force Base, Feb. 1954.

- 11. Parker, W. G., and Wolfhard, H. G.: Some Characteristics of Flames Supported by NO and NO<sub>2</sub>. Fourth Symposium (International) on Combustion, The Williams & Wilkins Co. (Baltimore), 1953, pp. 420-428.
- 12. Miller, Riley O.: Flame Propagation Limits of Propane and n-Pentane in Oxides of Nitrogen. NACA TN 3520, 1955.
- 13. Propulsion Engineering: Bimonthly Progress Report on the Improvement of White Fuming Nitric Acid. Rep. RE-16-12, North American Aviation, Inc., July 22, 1955. (Contract AF 33(616)-329.)
- 14. Special Products Research Department: Small Caliber High Performance Liquid Fueled Rocket Motor. Prog. Rep. No. 10, Rep. No. 80-4450R, Eclipse-Pioneer Div., Bendix Aviation Corp., July-Aug. 1954. (Contract No. W-30-069-ORD-4450R, Ord. Proj. TU2-7C.)
- 15. Kilpatrick, Martin, Baker, Louis L., Jr., and McKinney, C. Dana: Studies of Fast Reactions Which Evolve Gases. The Reaction of Sodium-Potassium Alloy with Water in the Presence and Absence of Oxygen. Jour. Phys. Chem., vol. 57, no. 4, Apr. 16, 1953, pp. 385-390.
- 16. Sutton, George P.: Rocket Propulsion Elements. John Wiley & Sons, Inc., 1949.
- 17. Ladanyi, Dezso J., and Miller, Riley O.: Comparison of Ignition Delays of Several Propellant Combinations Obtained with Modified Open-Cup and Small-Scale Rocket Engine Apparatus. NACA RM E53D03, 1953.
- 18. Carmody, D. R., and Zletz, A.: Development of Liquid Rocket Propellants. Final Rep., Standard Oil Co. (Ind.), May 15, 1954. (Contract AF-33(038)-22633.)
- 19. Strier, M., Felberg, R., and Pearl, C.: Investigation of the Relationship of Propellant Chemical Structure to Spontaneous Ignition with WFNA. Final Rep. No. RMI-466-F, Reaction Motors, Inc., Mar. 23, 1953. (Contract NOa(s)52-595-c.)

TABLE I. - ACID-FUEL RATIOS CORRESPONDING  $\mbox{TO VARIOUS} \quad \beta \quad \mbox{VALUES}$ 

Fuel	Aci β <sup>a</sup>	Acid-fuel ratio o/f f β <sup>a</sup> of -							
	0.55	0.65	0.80	1.00	1.25				
Hydrazine		0.96	1.18	1.48	1.85				
TMTP		1.82	2.24	2.80	3.50				
Furfuryl alcohol		1.85	2.28	2.85	3.56				
UDMH	1.86	2.20	2.70	3.38					
Allylamine	2.33	2.75	3.38	4.23					
o-Toluidine	2.41	2.85	3.50	4.38					

 $a \left[ \frac{(o/f)}{(o/f)_{stoichiometric}} \right]$ 

TABLE II. - BASIC EXPERIMENTAL DATA

[1-in.diam. chamber used except where noted]

					I-III. GIAIII.	Ortomo C.	abea .	orrocho ,	WILCI C HOUC	س]				
Chamber pressure, p <sub>c</sub> , lb/sq in. abs	Acid flow, Wo, lb/sec	Fuel flow, wf, lb/sec	Acid- fuel weight ratio, o/f	Charac- teristic exhaust velocity, c*, ft/sec	Chamber pressure, pc, lb/sq in. abs	W ,	Fuel flow, w <sub>f</sub> , lb/sec	Acid- fuel weight ratio, o/f	Charac- teristic exhaust velocity, c*, ft/sec	Chamber pressure, pc, lb/sq in. abs	Acid flow, Wo, lb/sec	Fuel flow, w <sub>f</sub> , lb/sec	Acid- fuel weight ratio, o/f	Charac- teristic exhaust velocity c*, ft/sec
					Hyd	razine;	A't = 0	.0882 sc	in.					
	L	*, 10 1	n.			L	*, 20 ir	1.			L.	*, 30 1r	1.	
201 206 207 235 254 267 261 247	0.055 .063 .069 .090 .109 .121 .126 .130	0.072 .068 .064 .064 .066 .061	0.77 .92 1.08 1.41 1.69 1.85 2.07 2.35	4510 4460 4410 4320 4170 4065 3985 3790	190 204 219 249 271 282 279 271	0.046 .056 .065 .083 .102 .114 .122	0.072 .067 .063 .063 .061 .061 .057	0.64 .83 1.02 1.33 1.67 1.89 2.13 2.43	4550 4720 4860 4810 4710 4570 4410 4200	192 207 227 246 266 279 276 266	0.049 .057 .067 .080 .094 .106 .113	0.071 .066 .064 .061 .061 .060 .057	0.69 .87 1.04 1.32 1.55 1.76 1.99 2.24	4560 4770 4930 4970 4895 4780 4610 4330
	L	*, 40 11	n.			L.	*, 50 ir					*, 75 ir		1000
218 228 256 270 270 282 277 262	0.058 .064 .080 .089 .094 .109 .116	0.074 .068 .067 .064 .062 .060 .057	0.78 .94 1.18 1.37 1.53 1.81 2.04 2.33	4695 4890 4950 5020 4920 4745 4540 4310	244 250 253 275 285 293 279 275	0.068 .073 .076 .089 .100 .109 .114	0.075 .071 .068 .067 .066 .063 .059	0.90 1.02 1.11 1.33 1.53 1.73 1.92 2.13	4880 4940 5000 4990 4890 4840 4580 4480	236 204 241 263 268 287 290 272	0.065 .058 .072 .085 .093 .106 .119	0.077 .069 .069 .066 .063 .063 .061	0.85 .85 1.05 1.29 1.47 1.69 1.94 2.11	4730 4570 4865 4940 4870 4820 4590 4390
	L4	*, 100	ln.											1000
237 235 248 257 253 268 283 278	0.068 .070 .078 .086 .089 .100 .118	0.076 .072 .070 .067 .063 .062 .062	0.90 .98 1.11 1.30 1.42 1.63 1.92 2.17	4665 4690 4770 4770 4720 4700 4470 4280										
				Tr	imethyl-tr	thiopho	osphite;	$A_t = 0$	0.0881 sq	in.				
	L.	*, 20 in	1.			L+	, 30 ir	1.			L,	, 40 ir	1.	
235 248 268 268 273 271 253 257	0.105 .112 .128 .130 .134 .141 .145	0.073 .070 .069 .064 .057 .050 .044 .043	1.44 1.60 1.85 2.03 2.35 2.81 3.30 3.67	3750 3865 3875 3925 4050 4030 3800 3620	242 259 271 273 274 274 259 265	0.104 .116 .125 .129 .134 .139 .143 .153	0.073 .072 .068 .063 .057 .051 .043	1.42 1.62 1.82 2.05 2.35 2.73 3.32 3.73	3880 3930 3990 4030 4075 4090 3970 3880	244 255 276 281 275 275 261 267	0.104 .113 .126 .131 .132 .137 .143	0.073 .072 .069 .063 .057 .052 .043	1.42 1.59 1.83 2.08 2.32 2.63 3.31 3.66	3910 3900 4020 4110 4130 4150 4010 3870
	L.	*, 50 ir	1.			L,	, 75 in				L*	, 100 1		
237 261 276 277 279 272 262 270	0.102 .114 .126 .129 .132 .136 .142	0.073 .072 .069 .064 .057 .050 .043	1.40 1.58 1.82 2.01 2.31 2.72 3.30 3.76	3840 3980 4040 4090 4210 4140 4010 3920	234 257 268 276 274 271 263 271	0.103 .117 .125 .131 .130 .135 .144	0.074 .071 .068 .063 .058 .051 .042	1.40 1.65 1.84 2.07 2.25 2.64 3.42 3.59	3750 3880 3940 4000 4130 4150 4010 3975	236 255 271 277 272 271 262 271	0.105 .118 .128 .133 .134 .138 .142	0.073 .071 .068 .063 .057 .050 .043	1.43 1.66 1.89 2.10 2.34 2.76 3.30 3.76	3770 3820 3940 4010 4050 4090 4030 3945

TABLE II. - Continued. BASIC EXPERIMENTAL DATA

[1-in. diam. chamber used except where noted]

Series of runs	Chamber pressure, p <sub>c</sub> , lb/sq in. abs	Acid flow, wo, lb/sec	Fuel flow, wf, lb/sec	Acid- fuel weight ratio, o/f	Charac- teristic exhaust velocity, c*, ft/sec	Chamber pressure, p <sub>c</sub> , lb/sq in. abs		Fuel flow, w <sub>f</sub> , lb/sec	0/1	Charac- teristic exhaust velocity, c*, ft/sec	Chamber pressure, Pc, lb/sq in. abs	Acid flow, w <sub>o</sub> , lb/sec	Fuel flow, wf, lb/sec	Acid- fuel weight ratio, o/f	Charac- teristic exhaust velocity, c*, ft/sec
					Fur	Furfuryl alcohol; $A_t = {}^{a}$ 0.0881 and ${}^{b}$ 0.0913 sq in.  L*. 30 in.  L*, 40 in.									
		L	*, 20 1	n.			L	*, 30 1	n.			Г.	*, 40 11	1.	
1	285 294 313 302 289 269 246 246	0.122 .129 .138 .142 .142 .148 .157 .165	0.078 .074 .073 .068 .059 .055 .049	1.57 1.76 1.89 2.09 2.41 2.69 3.20 3.37	4050 4120 4210 4080 4080 3760 3390 3260	296 310 330 312 303 286 260 271	0.118 .125 .136 .134 .140 .146 .150 .160	0.078 .075 .073 .065 .060 .053 .047	1.50 1.67 1.87 2.06 2.34 2.76 3.17 3.46	4290 4400 4490 4430 4300 4080 3740 3720	298 311 332 321 299 293 255 272	0.115 .124 .133 .134 .130 .136 .156	0.078 .074 .073 .066 .056 .051 .040	1.47 1.68 1.83 2.04 2.32 2.69 3.92 3.63	4390 4470 4590 4560 4560 4450 3700 3760
2	288 308 320 294 275 299 270 274	.129 .140 .150 .158 .163 .157 .162	.091 .092 .087 .083 .078 .064 .059	1.42 1.52 1.72 1.90 2.40 2.45 2.74 3.31	3850 3900 3970 3590 3355 3980 3590 3460	302 325 342 341 331 315 306 287	.124 .133 .142 .144 .148 .151 .153 .175	.090 .088 .084 .076 .069 .061 .055	1.38 1.51 1.69 1.89 2.14 2.48 2.78 3.43	4150 4320 4450 4560 4585 4370 4325 3730	294 321 339 332 327 324 314 302	.130 .133 .142 .147 .150 .152 .153 .172	.084 .079 .077 .070 .063 .059 .054	1.54 1.69 1.84 2.10 2.38 2.58 2.83 3.44	c 4040 c 4450 c 4550 4500 4510 4510 4460 4000
		L	*, 50 i	n.			L	*, 75 1	n.			L.	*, 100	in.	
1	258 275 321 312 306 303 285 287	0.096 .104 .130 .129 .133 .136 .142	0.084 .079 .074 .063 .057 .051 .041	1.15 1.32 1.76 2.05 2.34 2.67 3.44 3.89	C 4080 C 4280 C 4480 C 4600 C 4560 C 4600 C 4410 C 4215	302 310 328 328 309 307 289 280	0.119 .126 .131 .135 .137 .145 .146 .159	0.073 .070 .067 .060 .054 .049 .041	1.63 1.80 1.96 2.25 2.53 2.95 3.57 4.09	C 4430 C 4490 C 4700 C 4770 C 4590 4490 4390 4010	289 304 313 307 313 309 285 283	0.117 .126 .131 .134 .141 .142 .149	0.075 .071 .067 .060 .054 .049 .041	1.56 1.77 1.96 2.23 2.62 2.91 3.63 3.95	C4270 C4400 C4490 C4490 C4555 C4590 C4260 C4060
2	302 322 344 336 326 315 298 305	.123 .133 .141 .145 .147 .151 .159	.082 .080 .076 .069 .062 .054 .047	1.51 1.67 1.85 2.11 2.36 2.80 3.39 3.94	c 4330 c 4440 4660 4620 4590 4520 4250 c 4210	288 314 323 324 319 308 302 313	.121 .135 .144 .147 .149 .152 .156 .174	.069 .065 .064 .060 .056 .048 .045	1.76 2.08 2.26 2.44 2.68 3.14 3.50 4.00	c 4460 c 4620 c 4565 c 4600 c 4575 c 4530 c 4420 c 4220	288 306 326 322 308 305 285 268	.119 .131 .142 .143 .145 .149 .156	.077 .073 .071 .065 .056 .050 .041	1.54 1.79 1.99 2.21 2.61 3.01 3.78 4.61	c 4320 c 4410 c 4500 c 4550 c 4505 c 4510 c 4250 c 3630

<sup>&</sup>lt;sup>a</sup>First series of runs.

bSecond series of runs.

<sup>&</sup>lt;sup>c</sup>Audible scream.

TABLE II. - Continued. BASIC EXPERIMENTAL DATA

[1-in. diam. chamber used except where noted]

Series of runs	Chamber pressure, p <sub>c</sub> , lb/sq in. abs	Acid flow, Wo, lb/sec	Fuel flow, Wf, lb/sec	Acid- fuel weight ratio, o/f	Charac- teristic exhaust velocity, c*, ft/sec	Chamber pressure, p <sub>c</sub> , 1b/sq in. abs	Wo,	Fuel flow, Wf, lb/sec	Acid- fuel weight ratio, o/f	Charac- teristic exhaust velocity, c*, ft/sec	Chamber pressure, p <sub>c</sub> , lb/sq in. abs	W ,	Fuel flow, w <sub>f</sub> , lb/sec	Acid- fuel weight ratio, o/f	Charac- teristic exhaust velocity c*, ft/sec
				Uı	nsymmetric	al dimethy	lhydraz	ine; A <sub>t</sub>	= ao.o	892 and bo	.0866 sq 1	n.			
		L	*, 20 1	n.			L	*, 30 11	n.			L	*, 40 1	n.	
1	260 275 292 309 309 305 300 294	0.101 .109 .118 .133 .141 .145 .149 .155	0.065 .061 .061 .060 .056 .051 .046	1.55 1.79 1.93 2.22 2.52 2.84 3.24 3.88	4500 4645 4685 4600 4500 4470 4420 4330	262 281 296 315 320 318 308 303	0.097 .109 .117 .126 .139 .144 .146 .152	0.065 .061 .060 .057 .056 .050 .045	1.49 1.79 1.95 2.21 2.48 2.88 3.24 3.90	4640 4750 4800 4940 4710 4710 4630 4560	263 278 308 332 330 324 314 305	0.096 .105 .122 .036 .138 .141 .146 .152	0.065 .061 .061 .061 .055 .050 .044 .038	1.48 1.72 2.00 2.23 2.51 2.82 3.32 4.00	4690 4810 4830 4840 4910 4870 4750 4610
		I	*, 50 1	n.			L	*, 75 11	n.			L	*, 100	in.	
1	261 283 313 328 322 329 318 324	0.096 .107 .123 .130 .134 .141 .145 .150	0.064 .062 .062 .059 .055 .050 .044 .043	1.50 1.73 2.00 2.20 2.46 2.85 3.30 3.49	4680 4810 4860 4980 4890 4970 4830 4820	266 282 324 340 326 335 324 316	0.099 .108 .128 .137 .135 .142 .146 .153	0.065 .062 .062 .059 .053 .049 .043	1.52 1.74 2.06 2.32 2.55 2.90 3.40 4.03	4660 4760 4900 4980 4980 5040 4920 4750	259 295 314 323 336 330 323 314	0.099 .115 .127 .132 .141 .140 .145 .153	0.066 .064 .061 .059 .054 .049 .043	1.50 1.80 2.08 2.24 2.61 2.86 3.37 4.14	4510 4730 4800 4860 4950 5010 4930 4750
2	7250 1050 5.110 1020			282 321 298 323 339 332 316 318	.105 .122 .115 .126 .138 .141 .148 .166	.062 .062 .055 .054 .052 .046 .038	1.69 1.97 2.09 2.33 2.65 3.07 3.89 4.74	4710 4860 4885 5000 4970 4950 4730 4410	284 299 321 327 339 329 314 316	.108 .117 .126 .130 .139 .140 .150 .163	.064 .060 .059 .057 .052 .046 .038	1.69 1.95 2.14 2.28 2.67 3.04 3.95 4.66	4600 4710 4835 4870 4945 4930 4655 4450		
					Allyl	amine; A <sub>t</sub>	= °0.09	05, do.	0864, a	nd <sup>e</sup> 0.0872	sq in.				
		L	*, 20 1	n.			L	*, 30 1	n.			L	*, 40 1	n.	
1	365 359 349 307 295 275	0.165 .171 .175 .190 .193 .200	0.085 .078 .069 .056 .054 .049	1.94 2.21 2.55 3.42 3.57 4.08	4250 4210 4175 3640 3480 3220	373 369 358 347 320 309 287	0.164 .170 .175 .183 .192 .193 .200	0.087 .076 .068 .060 .053 .050	1.90 2.24 2.60 3.07 3.62 3.86 4.35	4330 4370 4300 4180 3805 3700 3600	379 372 364 358 333 321 300	0.163 .166 .171 .178 .186 .188 .198	0.084 .075 .067 .058 .052 .049	1.95 2.21 2.55 3.07 3.61 3.88 4.50	4480 4500 4460 4420 4090 3955 3610
		L	*, 50 1	n.			L	*, 75 1	n.			L	*, 100	in.	
2	397 387 378 366 348 334 319	0.161 .158 .165 .172 .184 .192 .196	0.083 .072 .063 .053 .048 .042	1.95 2.19 2.62 3.24 3.87 4.57 5.03	4535 4675 4610 4520 4180 3970 3770	394 391 385 378 362 344 339	0.159 .160 .165 .169 .181 .189 .184	0.078 .070 .060 .053 .045 .040	2.05 2.29 2.75 3.21 4.02 4.73 4.84	4630 4730 4750 4750 4460 4180 4250	402 396 387 378 368 356 340	0.160 .160 .162 .168 .180 .182 .188	0.081 .073 .060 .049 .042 .040	1.98 2.21 2.70 3.43 4.30 4.61 5.22	4640 4740 4850 4850 4600 4510 4255
3	374 383 366 317	.167 .179 .187 .195	.063 .058 .049	2.63 3.07 3.80 4.86	4560 4530 4350 3790										

aFirst series of runs for UDMH.

bSecond series of runs for UDMH.

<sup>&</sup>lt;sup>C</sup>First series of runs for allylamine.

dSecond series of runs for allylamine.

eThird series of runs for allylamine.

TABLE II. - Continued. BASIC EXPERIMENTAL DATA

[1-in.diam.chamber used except where noted]

Chamber pressure, pc, lb/sq in. abs	wo,	Fuel flow, w <sub>f</sub> , lb/sec		Characteristic exhaust velocity, c*, ft/sec	Chamber pressure, p <sub>c</sub> , lb/sq in. abs	W 0,	Fuel flow, w <sub>f</sub> , lb/sec	Acid- fuel weight ratio, o/f	Charac- teristic exhaust velocity, c*, ft/sec	Chamber pressure, Pc, lb/sq in. abs	Acid flow, w <sub>o</sub> , lb/sec	Fuel flow, w <sub>f</sub> , lb/sec	Acid- fuel weight ratio, o/f	Charac- teristic exhaust velocity, c*, ft/sec
					<u>o</u> -To	ludine;	A <sub>t</sub> = 0	.0920 s	q in.					
	L	, 30 in	n.			L	*, 40 1	n.			L	*, 50 11	n.	
337 336 330 324 311 311 304	0.162 .166 .171 .176 .182 .196 .203	0.093 .083 .072 .062 .053 .052	1.75 2.00 2.39 2.83 3.43 3.77 4.32	3920 4000 4030 4040 3920 3720 3600	350 345 334 333 316 314 313	0.159 .164 .167 .174 .180 .190 .206	0.091 .080 .072 .062 .053 .049	1.74 2.05 2.32 2.82 3.43 3.88 4.48	4160 4190 4140 4175 4030 3890 3680	350 357 345 312 300 348 345	0.155 .160 .167 .177 .211 .157 .162	0.086 .078 .069 .049 .039 .091	1.80 2.05 2.42 3.61 5.41 1.73 2.03	4300 4440 4330 4090 3550 4160 4225
	L	*, 75 11	n.			L	*, 100	in.		342	.167	.071	2.35	4260
356 319 339 349	0.157 .139 .155 .171	0.088 .090 .074 .059	1.78 1.54 2.09 2.90	4310 4130 4390 4500	354 364 349 360	0.158 .163 .163	0.088 .079 .066 .057	1.80 2.06 2.47 2.96	a4265 4460 a4520 4720	331 324 324 317	.172 .177 .190 .209	.060 .052 .047 .044	2.87 3.40 4.04 4.75	4230 4190 4050 3710
340 344 343	.176 .187 .205	.049 .044 .038	3.63 4.25 5.39	4480 4410 4180	346 358 345	.175 .188 .211	.046 .044 .033	3.80 4.27 6.39	4640 4570 4190					
				Hydr	azine; 1.5	-indi	am.cham	bers; A	t = 0.0848	sq in.				
	L	*, 33 11	n.			L	*, 50 1	n.				*, 75 1		
245 240 239 257 260 276 269 282	0.062 .066 .074 .081 .092 .104 .113	0.076 .070 .062 .065 .061 .061 .057	0.82 .94 1.19 1.25 1.50 1.71 1.98 2.28	4860 4810 4810 4810 4630 4565 4340 4225	234 253 250 261 274 284 300 297	0.058 .068 .068 .079 .092 .102 .121 .130	0.075 .070 .066 .062 .061 .061 .060	0.77 .96 1.03 1.27 1.50 1.68 2.02 2.27	4780 5010 5060 5050 4860 4770 4520 4325	225 241 247 270 306 312 316 306	0.058 .065 .069 .083 .101 .113 .125 .132	0.075 .070 .067 .064 .066 .064 .061	0.77 .92 1.03 1.31 1.52 1.77 2.04 2.31	4630 4890 4940 5015 5000 4830 4620 4400
	L	*, 100	in.			L	*, 144	in.						
241 231 231 250 279 317 286 285	0.063 .062 .067 .077 .091 .119 .120	0.076 .070 .065 .062 .062 .064 .057	0.83 .90 1.01 1.25 1.48 1.86 2.11 2.36	4750 4770 4780 4910 4980 4720 4410 4210	230 229 232 264 273 300 274 290	0.060 .065 .069 .084 .092 .110 .114 .126	0.074 .069 .065 .065 .062 .063 .056	0.80 .94 1.06 1.30 1.50 1.75 2.05 2.21	4710 4680 4700 4860 4850 4760 4410 4320					
				Hydr	azine; 2-1				= 0.0848 s	q in.				
	_	*, 50 1	_			т	*, 75 1	_			_	*, 100	_	1000
238 233 234 257 269 272 291 285	0.064 .067 .068 .088 .103 .109 .128	0.074 .069 .065 .064 .062 .060 .060	0.86 .97 1.05 1.38 1.66 1.82 2.13 2.36	4700 4680 4810 4615 4440 4390 4220 4140	237 236 255 273 262 263 299 295	0.060 .062 .072 .085 .087 .093 .117 .126	0.074 .071 .068 .066 .061 .061 .061	0.82 .87 1.06 1.29 1.42 1.54 1.92 2.20	4820 4840 4950 4900 4820 4695 4570 4390	255 244 261 270 296 308 289 297	0.066 .065 .074 .081 .098 .109 .110	0.076 .072 .069 .067 .066 .065 .059	0.87 .90 1.08 1.22 1.50 1.69 1.84 2.09	4920 4880 4960 4970 4940 4850 4660 4560
	_	*, 171	_			_	*, 300	i						
242 241 256 252 269 313 288 288	0.064 .065 .073 .078 .092 .113 .118	0.076 .071 .069 .064 .060 .065 .060	0.83 .91 1.06 1.21 1.53 1.73 1.97 2.17	4715 4835 4920 4825 4810 4800 4430 4330	244 242 251 276 286 278 297 284	0.066 .067 .073 .089 .096 .105 .118 .126	0.077 .073 .068 .066 .064 .059 .061	0.85 .92 1.07 1.35 1.50 1.80 1.92 2.25	4640 4715 4840 4860 4880 4630 4540 4250					

aAudible scream.

TABLE II. - Concluded. BASIC EXPERIMENTAL DATA

[1-in. diam. chamber used except where noted]

Chamber pressure, p <sub>c</sub> , lb/sq in. abs	Acid flow, w <sub>o</sub> , lb/sec	Fuel flow, w <sub>f</sub> , lb/sec	Acid- fuel weight ratio, o/f	Charac- teristic exhaust velocity c*, ft/sec	Chamber pressure, pc, lb/sq in. abs	Acid flow, Wo, lb/sec	Fuel flow, w <sub>f</sub> , lb/sec	Acid- fuel weight ratio, o/f	Charac- teristic exhaust velocity, c*, ft/sec	Chamber pressure, pc, lb/sq in. abs	Acid flow, Wo, lb/sec	Fuel flow, w <sub>f</sub> , lb/sec	Acid- fuel weight ratio, o/f	Charac- teristic exhaust velocity c*, ft/sec
			Unsym	metrical d	imethylhyd	razine;	1.5-in	diam.	chambers;	$A_{t} = 0.085$	0 sq in			
	L.	*, 33 1:					, 50 1					*, 75 1:	n.	
262 283 297 330 326 324 314 308	0.094 .107 .117 .136 .138 .142 .146 .153	0.066 .062 .061 .061 .056 .051 .046	1.42 1.73 1.92 2.23 2.46 2.78 3.17 3.92	4480 4580 4570 4580 4600 4590 4480 4390	269 286 308 331 337 332 325 315	0.095 .103 .114 .127 .134 .138 .142 .150	0.064 .062 .060 .059 .055 .050 .045	1.48 1.66 1.90 2.15 2.44 2.76 3.16 4.05	4630 4740 4840 4870 4880 4830 4760 4610	274 301 333 359 349 342 333 323	0.094 .107 .123 .136 .134 .138 .141	0.066 .062 .062 .060 .055 .049 .043	1.43 1.73 1.98 2.26 2.44 2.82 3.28 4.06	4690 4880 4930 5010 5050 5010 4950 4730
					235 261 279 311 337 333 325 316	.081 .091 .099 .115 .135 .139 .144	.068 .065 .063 .061 .055 .050 .044	1.19 1.40 1.57 1.89 2.46 2.78 3.27 4.03	4320 4580 4710 4840 4855 4820 4730 4530					
	L*	, 100 1	ln.			L*	, 144 1	n.						
270 311 316 329 347 345 336 325	0.096 .112 .116 .123 .133 .138 .143 .151	0.065 .064 .060 .058 .055 .049 .043	1.48 1.75 1.93 2.12 2.42 2.82 3.32 4.08	4590 4840 4910 4975 5050 5050 4940 4730	270 294 314 336 345 343 334 325	0.096 .107 .117 .128 .133 .136 .141 .149	0.066 .063 .061 .060 .055 .049 .043	1.45 1.70 1.92 2.13 2.42 2.78 3.28 4.03	4560 4730 4830 4890 5020 5075 4970 4780					
			Unsymm	etrical di	Lmethylhydr	azine;	2-ind	liam.cha	mbers; At	= 0.0850 s	q in.			
	L*	, 50 ir	1.			L*	, 75 ir				L+	*, 100 i	in.	7700
257 280 309 329 322 316 307 303	0.097 .109 .126 .136 .139 .141 .145	0.067 .064 .063 .063 .056 .051 .046	1.45 1.70 2.00 2.16 2.48 2.76 3.15 3.80	4290 4430 4475 4525 4520 4505 4400 4320	261 294 312 329 340 338 328 315	0.091 .107 .117 .126 .135 .137 .141	0.065 .062 .061 .059 .055 .050 .044	1.40 1.73 1.92 2.14 2.45 2.74 3.20 3.95	4580 4760 4800 4870 4900 4950 4850 4590	265 296 326 359 342 348 340 328	0.090 .105 .119 .134 .130 .138 .143 .152	0.064 .061 .060 .060 .053 .048 .041	1.41 1.72 1.98 2.23 2.45 2.88 3.49 4.22	4710 4880 4980 5060 5115 5120 5060 4775
-	L*	, 171 1	n.			L*	, 300 1	n.						
268 280 322 347 351 345 337 324	0.097 .104 .119 .131 .135 .139 .142	0.064 .062 .062 .060 .054 .048 .043 .037	1.52 1.68 1.92 2.18 2.50 2.90 3.30 4.11	4430 4620 4870 4970 5080 5050 4985 4690	259 287 305 349 344 341 332 318	0.097 .110 .119 .136 .136 .140 .144 .152	0.065 .062 .060 .061 .054 .049 .043	1.49 1.77 1.98 2.23 2.52 2.86 3.35 4.11	4375 4570 4660 4845 4955 4940 4860 4605					

TABLE III. - FUEL RATINGS; CHARACTERISTIC LENGTH

 $L_{97}^{*}$  AS FUNCTION OF  $\beta$ 

Fuel	Stoichiometric		L*97	for β	of -	
	o/f ratio	0.55	0.65	0.80	1.00	1.25
Hydrazine	1:48		16.0	19.0	19.5	19.5
TMTP	2.80		24.0	27.5	21.5	25.0
Furfuryl alcohol	2.85		25.0	31.0	40.0	48.0
UDMH	3.38	24.5	28.5	37.0	42.5	
Allylaminea	4.23	54.0	60.0	75.0	84.0	
o-Toluidinea	4.38	75.0	80.0	83.0	76.0	

aMinimum values based on c\* at an L\* of 100 in.

TABLE IV. - MAXIMUM EXPERIMENTAL VALUES FOR

# CHARACTERISTIC EXHAUST VELOCITY c\*

Fuel		c* f	or β	of -	
	0.55	0.65	0.80	1.00	1.25
Hydrazine		4900	5010	4940	4720
TMTP		4050	4190	4160	3990
Furfuryl alcohol		4530	4600	4570	4400
UDMH	4870	4960	5010	4940	
Allylaminea	4790	4860	4860	4650	
o-Toluidine <sup>a</sup>	4590	4680	4700	4550	

avalues at an L\* of 100 in.

TABLE V. - CHARACTERISTIC LENGTH L97

# AS FUNCTION OF CHAMBER DIAMETER

Fuel	Diameter,	L*97		β
	111.	of		- 00
		0.65	0.80	1.00
Hydrazine	1.0 1.5 2.0	16.0 36.5 50.0	19.0 36.0 56.5	19.5 39.0 76.0
UDMH	1.0 1.5 2.0	28.5 49.5 78.0	37.0 56.0 75.0	42.5 60.0 84.0

TABLE VI. - CORRELATION OF CHARACTERISTIC LENGTH L\* FOR VARIOUS CHAMBER DIAMETERS

Fuel	$L_{97}^{*}(1.5-in. diam) - L_{97}^{*}(1.0-in. diam)$									
		β		Average						
	0.65	0.80	1.00	difference						
Hydrazine UDMH	20.5	17.0 19.0	19.5 17.5	19.0 19.2						
	L <sub>97</sub> (2-in	L*(2-in. diam) - L*(1.0-in. dia								
Hydrazine UDMH	34.0 49.5	37.5 38.0	56.5 41.5	42.7 43.0						

TABLE VII. - COMPARISON OF CHARACTERISTIC LENGTH Ly, CUP PRESSURE DROP, AND IGNITION DELAY VALUES

Fuel	L** a, in.	Cup pressure drop, lb/sq in.	Ignition delay, millisec
Hydrazine TMTP Furfuryl alcohol UDMH Allylamine o-Toluidine	16	305	<sup>b</sup> 6
	24	129	<sup>c</sup> 7.6
	25	81	<sup>d</sup> 25
	28.5	124	<sup>e</sup> 2
	f60	100	<sup>d</sup> 310
	f80	88	<sup>d</sup> 350

aTaken at  $\beta$  of 0.65.

bwith WFNA, 70° F, ref. 17.

CWith RFNA (18 percent NO<sub>2</sub>), -40° F, ref. 18.

dWith WFNA, 70° F, ref. 19.

eWith RFNA, -65° to 70° F, ref. 10.

fMinimum values based on c\* at an L\* of 100 in.

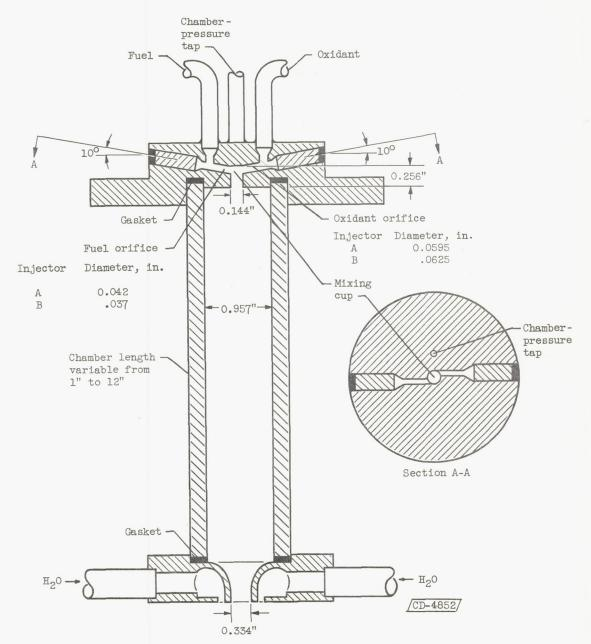


Figure 1. - Cross section of rocket-engine assembly.

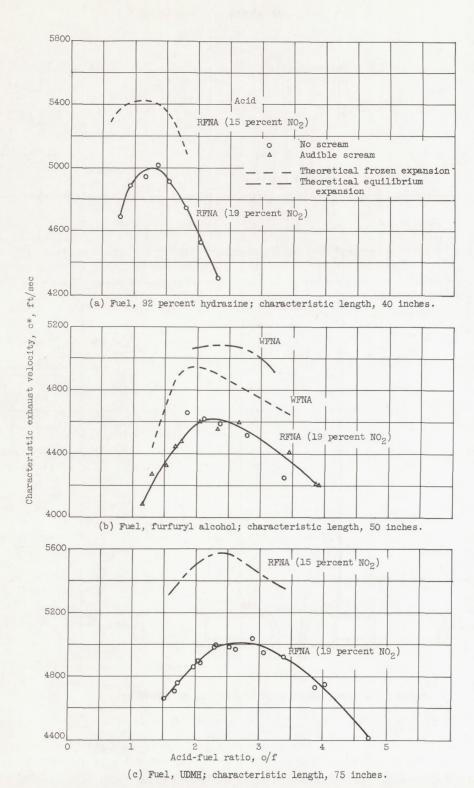
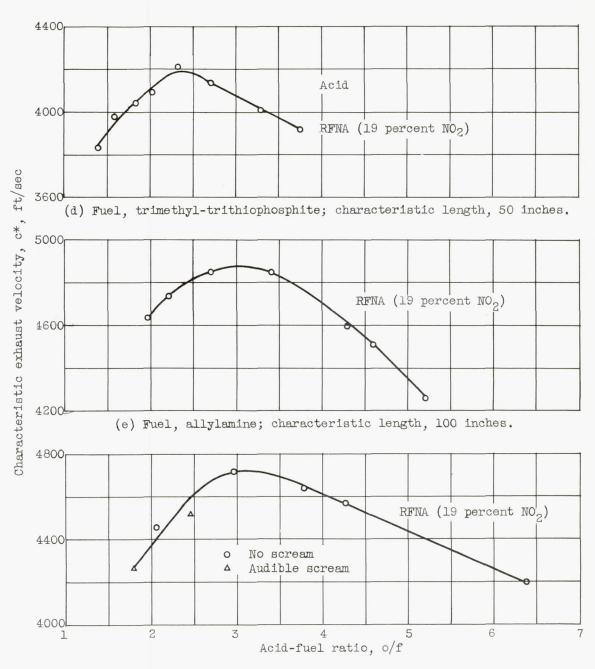


Figure 2. - Characteristic exhaust velocity as function of acid-fuel ratio at characteristic length of maximum experimental characteristic exhaust velocity.



(f) Fuel, o-toluidine; characteristic length, 100 inches.

Figure 2. - Concluded. Characteristic exhaust velocity as function of acid-fuel ratio at characteristic length of maximum experimental characteristic exhaust velocity.

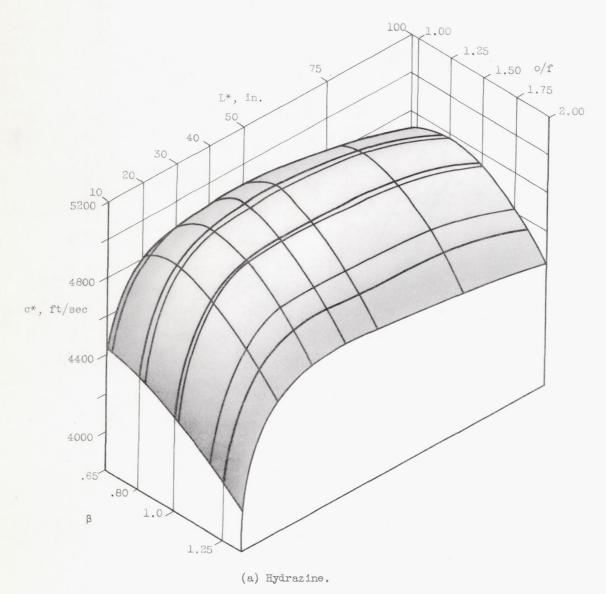
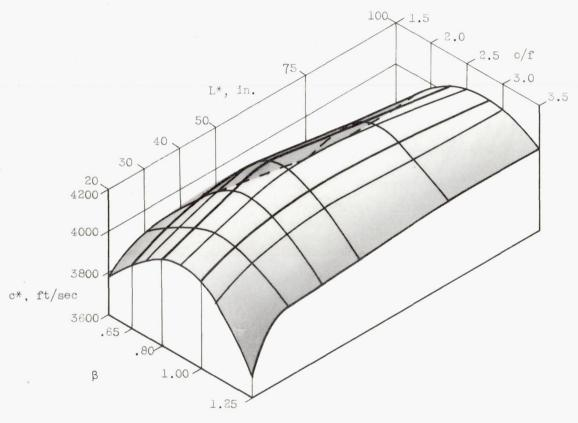


Figure 3. - Characteristic exhaust velocity c\* as function of characteristic length L\* and acid-fuel ratio o/f in 1-inch-diameter chambers.



(b) Trimethyl-trithiophosphite.

Figure 3. - Continued. Characteristic exhaust velocity c\* as function of characteristic length  $L^*$  and acid-fuel ratio o/f in l-inch-diameter chambers.

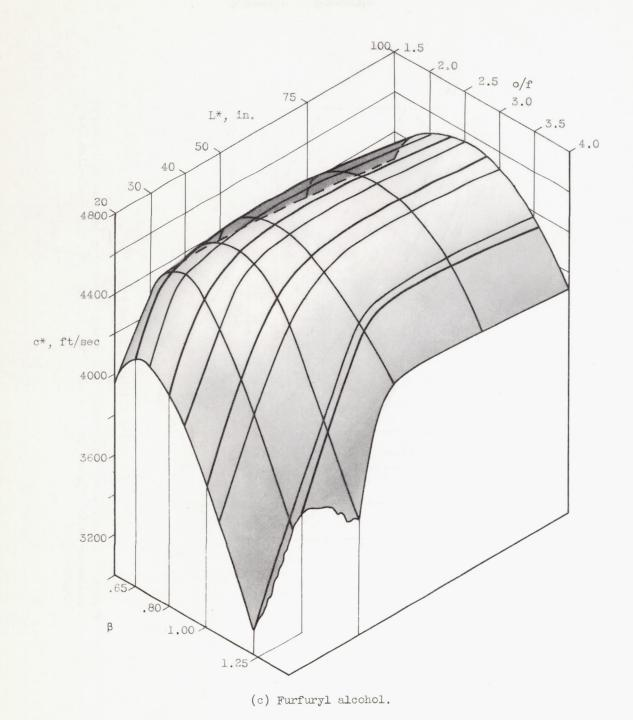
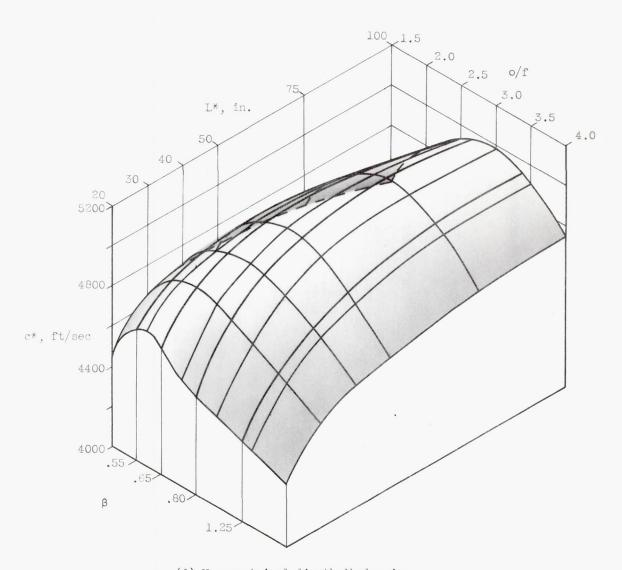


Figure 3. - Continued. Characteristic exhaust velocity c\* as function of characteristic length L\* and acid-fuel ratio o/f in l-inch-diameter chambers.



(d) Unsymmetrical dimethylhydrazine.

Figure 3. - Continued. Characteristic exhaust velocity c\* as function of characteristic length  $L^*$  and acid-fuel ratio o/f in l-inch-diameter chambers.

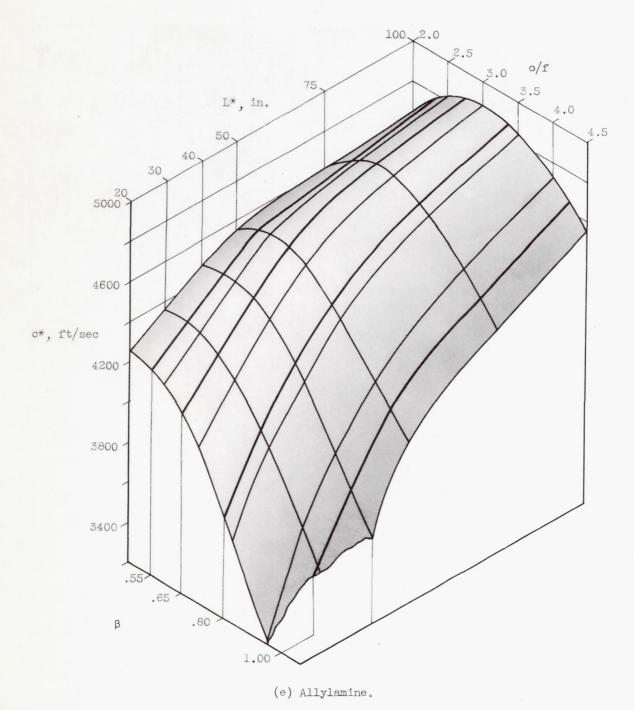


Figure 3. - Continued. Characteristic exhaust velocity c\* as function of characteristic length  $L^*$  and acid-fuel ratio o/f in l-inch-diameter chambers.

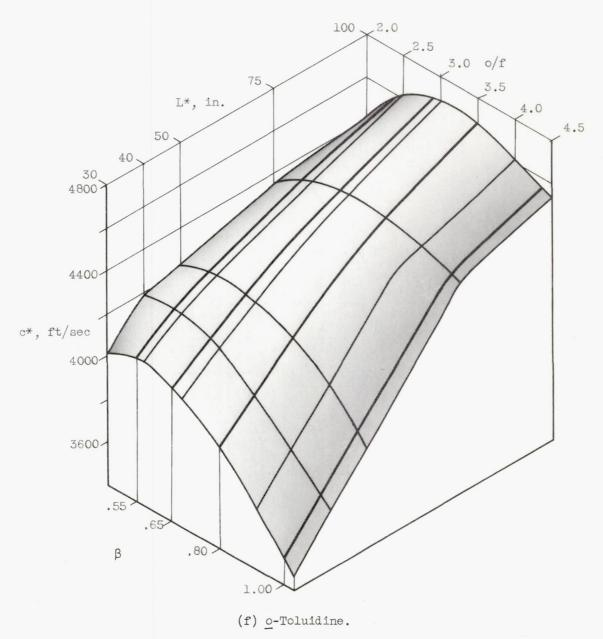


Figure 3. - Concluded. Characteristic exhaust velocity c\* as function of characteristic length L\* and acid-fuel ratio o/f in l-inch-diameter chambers.

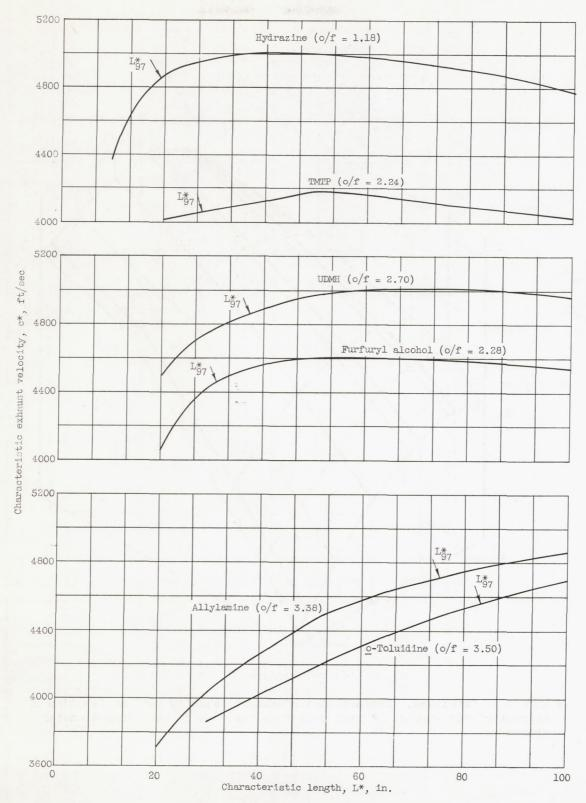


Figure 4. - Comparison of fuels at a  $\beta$  of 0.80.

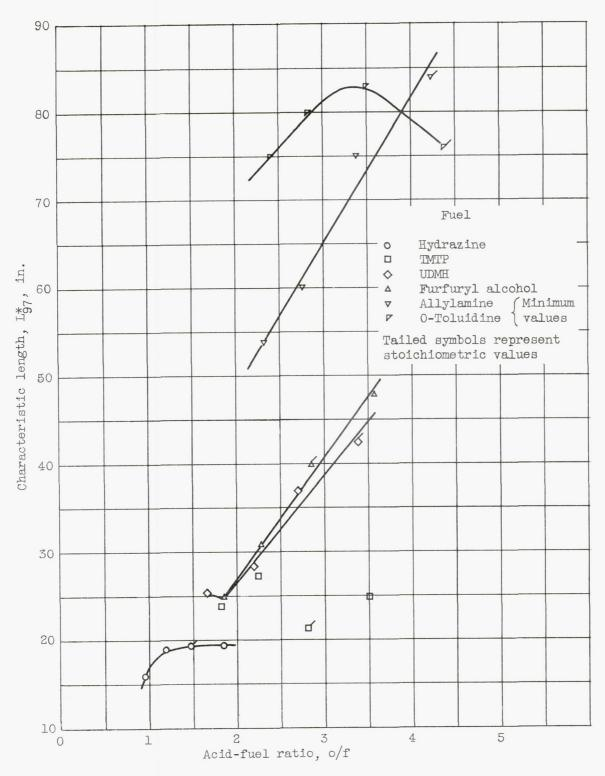


Figure 5. - Effect of stoichiometry;  $L_{97}^*$  as function of acid-fuel ratio.

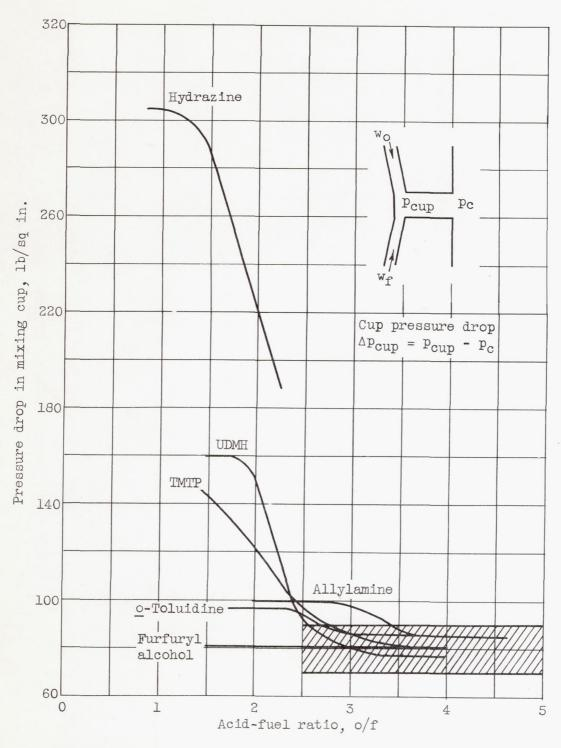
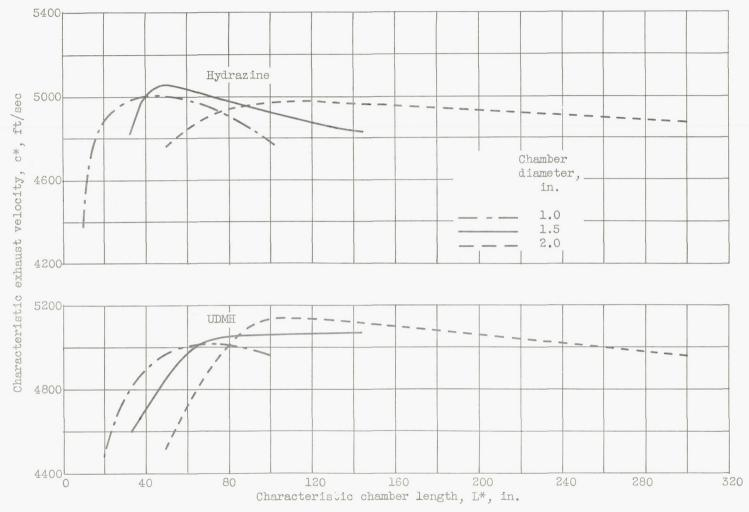
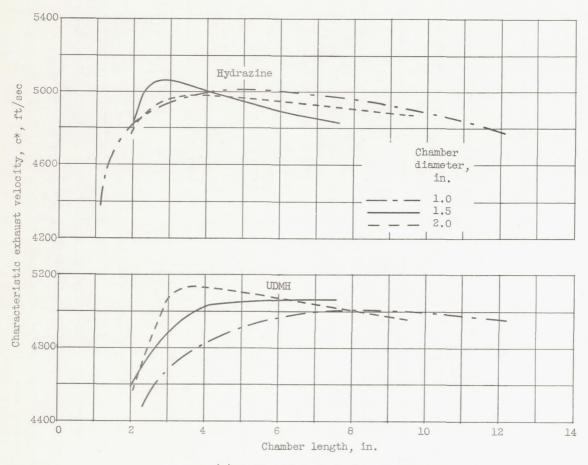


Figure 6. - Cup pressure drop reduced to uniform flow rate ( $w_{\rm T}$  = 0.2 lb/sec) as function of acid-fuel ratio.



(a) As function of characteristic length.

Figure 7. - Effect of chamber diameter on characteristic exhaust velocity  $\,c^*\,$  at a  $\,\beta\,$  of 0.80.



(b) As function of chamber length.

Figure 7. - Concluded. Effect of chamber diameter on characteristic exhaust velocity c\* at a  $\beta$  of 0.80.

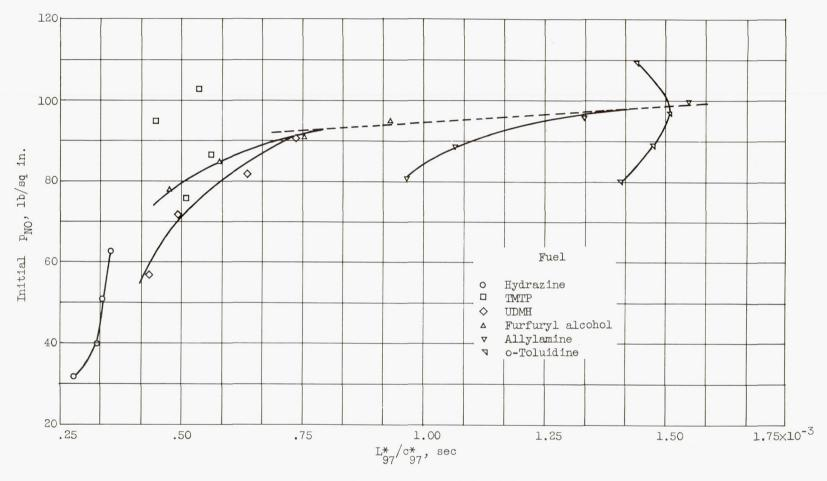


Figure 8. - Correlation of reactivity with initial NO concentration.

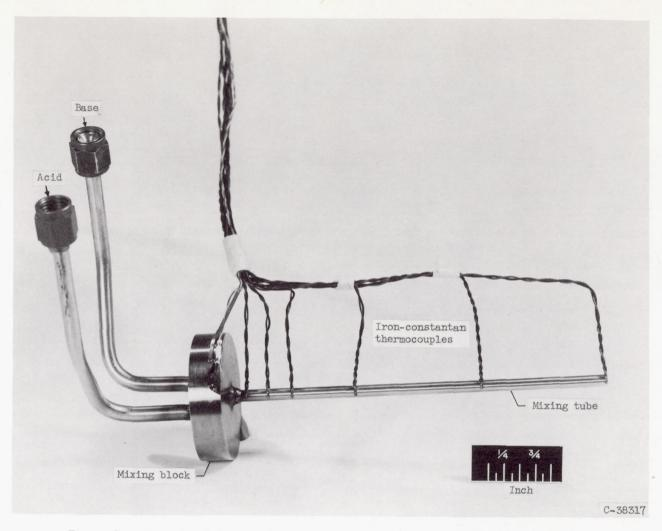


Figure 9. - Experimental apparatus for determining mixing efficiency of injectors.

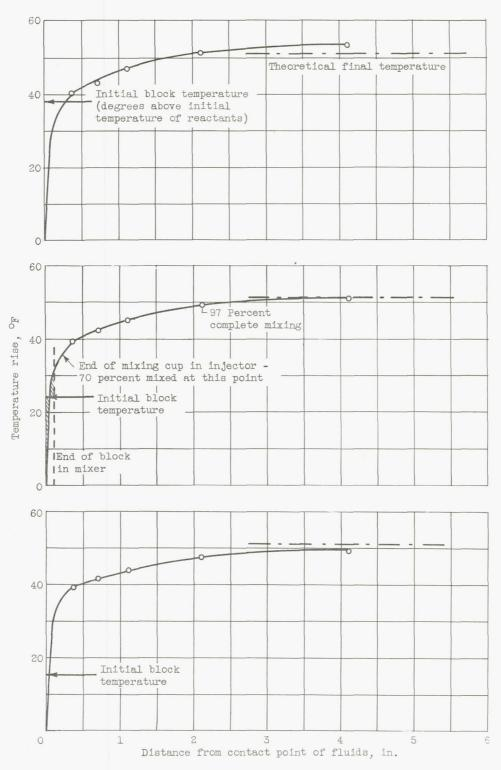


Figure 10. - Temperature rise as function of distance along mixer for three initial block temperatures.

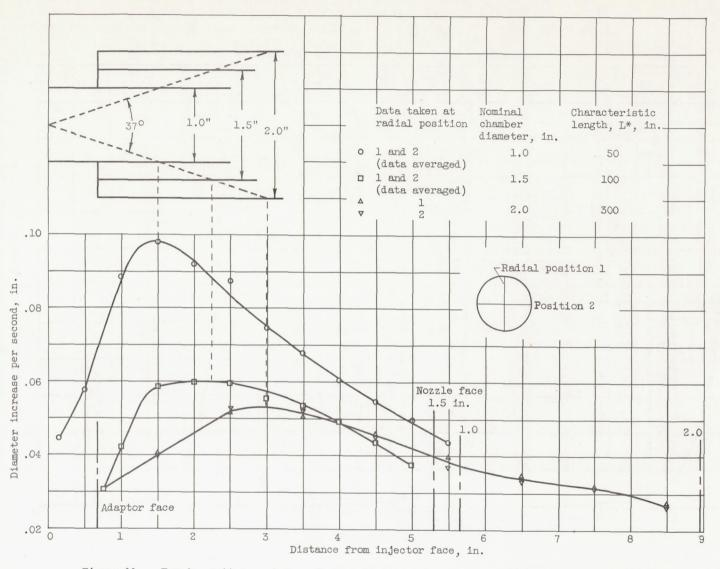


Figure 11. - Erosion pattern and its relation to diameter and chamber geometry. Fuel, hydrazine.



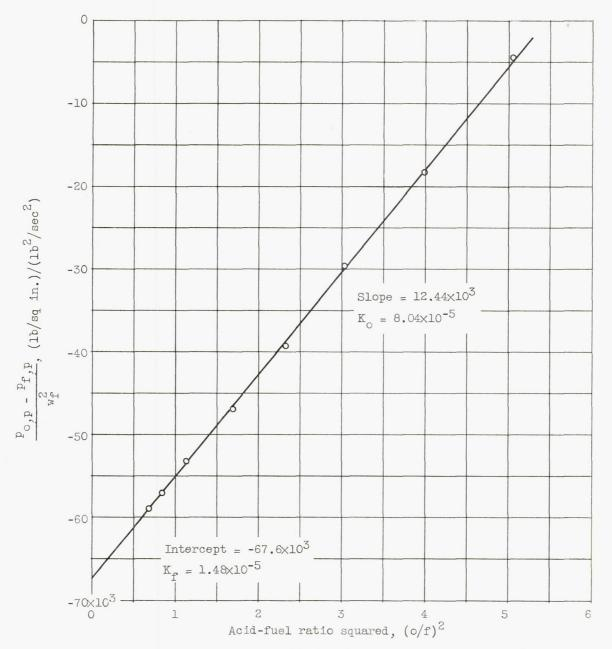


Figure 12. - Example of graphical calculation of flow constants  $\rm\,K_{\odot}\,$  and  $\rm\,K_{f}\,$  for hydrazine.